PHYSICAL CHEMISTRY CHEMICAL PHYSIC

Systematically Investigate Mechanical, Electronic, and Interfacial Properties of High Mobility Monolayer InAs from First-Principles Calculations

Wenjing Yu, [1,2] Jingzhen Li,[2*] Yi Wu, [1,2] Jing Lu, [3] Yongzhe Zhang[1,2*]

[1] Faculty of Materials and Manufacturing, Beijing University of Technology, Beijing, 100124, China

[2] Key Laboratory of Optoelectronics Technology of Education Ministry of China, Faculty of Information Technology, Beijing University of Technology, Beijing 100124, China.

[3] State Key Laboratory of Mesoscopic Physics and Department of Physics, Peking University, Beijing 100871, P. R. China

* Corresponding author. Email: yzzhang@bjut.edu.cn, jzli11@bjut.edu.cn

1. Supplementary Figure

The ML hydrogenated passivated InAs is a direct band gap semiconductor with a band gap of 1.70 eV calculated by the hybridization generalization (HSE06) as shown in **Fig. S1.** and the band gap of 1.59 eV was calculated by PBE in the manuscript. The difference between the results calculated by the two methods is 0.11 eV. Moreover, the conduction band minimum and valence band maximum of the 2D ML hydrogenated passivated InAs are located at the high symmetry point Γ point. We also give the electronic states which near the Fermi energy level are mainly from the orbital contributions of the As atoms.

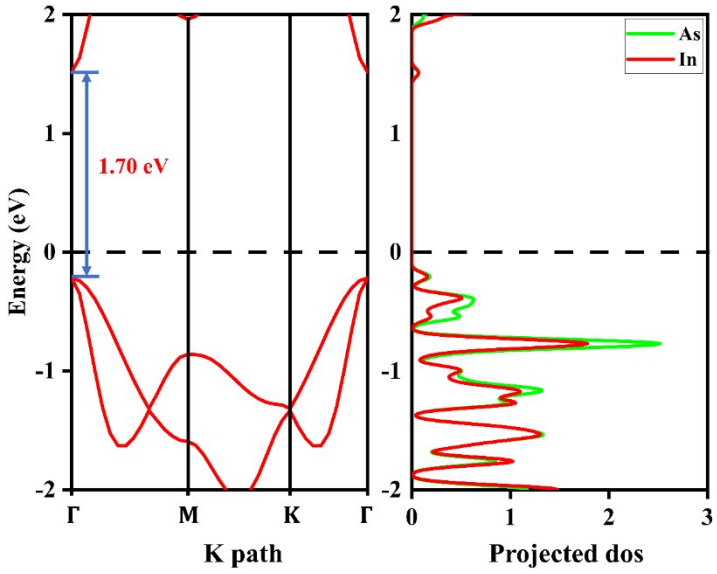

Fig. S1 Energy bands and density of states of ML hydrogenated passivated InAs calculated by the hybridization generalization (HSE06).

The convex hull energy phrase diagram is used to further verify the thermodynamic stability of InAs material, as shown in **Fig. S2**.**[1]** By comparing the position of the target compound relative to the red dashed line, if it is above the red dashed line it is likely to decompose (e.g., A in the inset of Fig. S2, which would decompose into In and As) or be in a sub-stable state; if it is below the red dashed line (e.g., B in the inset of Fig. S2), the compound is stable. As noticed, the convex hull energy is below the red dashed line indicating that the InAs is thermodynamically stable.

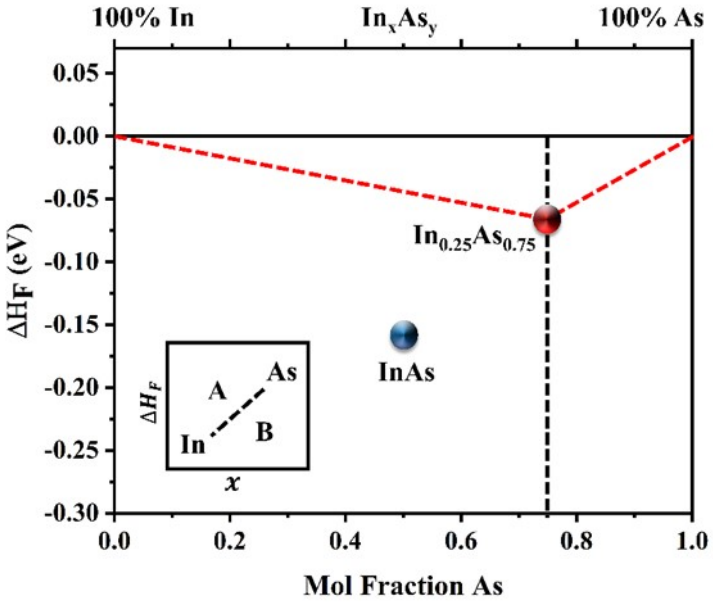

Fig. S2 Calculated the convex hull phrase diagram of InAs

The thermodynamic stability of the InAs material is demonstrated by the given binary phase diagram of In-As containing the stable compound InAs, as shown in **Fig. S3**.

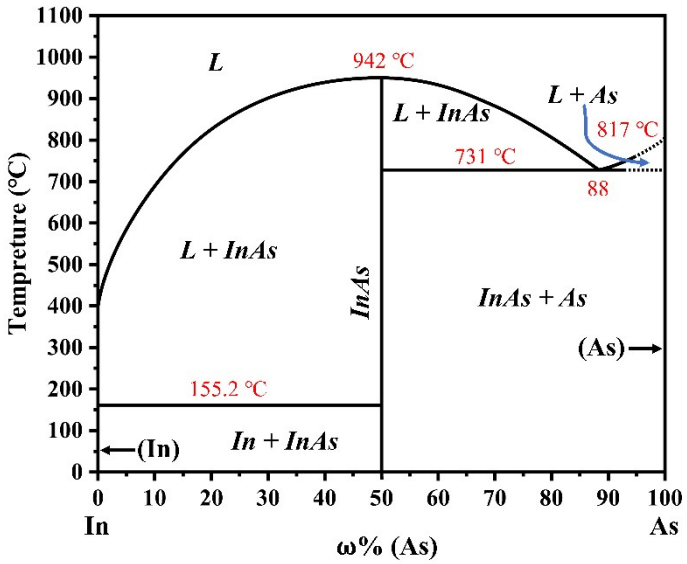

Fig. S3 Binary phase diagram of In-As containing the stable compound InAs.

we have obtained the thermoelectric parameters, seebeck coefficients (*S*), versus chemical potential (μ) and temperature (T) for the relaxation time approximation by solving the semiclassical Boltzmann transport equation in the BoltzTrap program as shown in **Fig. S4**.

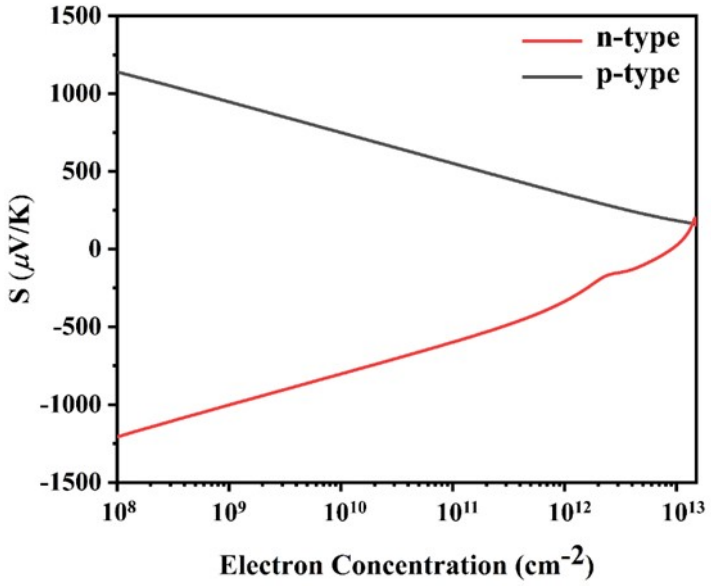

Fig. S4 Seebeck coefficient (*S*) as a function of carrier concentration at 300K for the ML hydrogenated passivated InAs.

The absolute |S| is exhibits weak anisotropy. The p-type |*S*| value is 546 $\mu V/K$ at 300 K when the carrier concentration is $1 \times 10^{11}\ cm^{-2}$ and the n-type |*S*| value is 606 $\mu V/K$ higher than the p-type. It's noted that the S is determined by the electronic structure. The novel method proposed in Ref **[2]** starts by setting the Seebeck coefficient S as an input to determine the reduced chemical potential η_{eff} from its definition in BoltzTraP.

$$S = \frac{k_B 2 + \lambda F_{1+\lambda}(\eta_{eff})}{q\ 1+\lambda\ \ F_\lambda(\eta_{eff})} - \eta_{eff} \#(1)$$

$F_{1+\lambda}$ are the fermi function given by the following expression:

$$F_j(\eta) = \int_0^\infty \frac{e^j d\varepsilon}{1 + e^{\varepsilon - \eta}} \#(2)$$

The fundamental difference between the deformation potential theory **(method 1)** approach and the novel method proposed in refer 1 **(method 2)** is the effective mass (m^*_s). We then attain the effective mass m^*_s in the following expression:

$$n = \frac{1}{2\pi^2}\left(\frac{2m^*_s k_B T}{\hbar^2}\right)^{3/2} F_{1/2}(\eta_{eff}) \#(3)$$

Based on the calculated concentration to obtain the effective mass (m^*_s). In this work, the effective mass is 0.15 m_0 calculated by the method 1 and 0.62 m_0 calculated by the method 2, where m_0 is

the electron rest mass ($m_0 = 9.11 \times 10^{-31}$). The carrier mobility was calculated to be 28 $cm^2\ V^{-1}\ s^{-1}$ which is now in the same order of magnitude with the experimental value**[3]** of 25 $cm^2\ V^{-1}\ s^{-1}$ as shown in **Table S1.**

Table S1 Calculations of the carrier mobility of 2D $InAsH_2$ at room temperature. m* represents the effective mass of ML $InAsH_2$ in the carrier transport direction. C_{2D} represents the modulus of elasticity of ML $InAsH_2$. E_1 presents the carrier deformation potential constant of the ML $InAsH_2$. μ is the carrier mobility of ML $InAsH_2$.

method	carrier type	$m^*(m_0)$	C_{2D} (J/m^2)	$E_1(eV)$	μ_{calcu} $(cm^2V^{-1}s^{-1})$	μ_{expe} $(cm^2V^{-1}s^{-1})$
method 1	electrons	0.15	37.426	7.57	490	25
	holes	1.00	37.426	3.39	155	25
method 2	electrons	0.62	37.426	3.39	28	25

Since Pt and Pd are heavy elements, they contain large spin-orbit coupling effects**[4]**, we recalculated the energy band structure of the system of InAs with metal Pd interfaces considering the spin-orbit coupling effect as shown in **Fig. S5**. The results of the projected energy bands show that the SOC affects the band structure slightly.

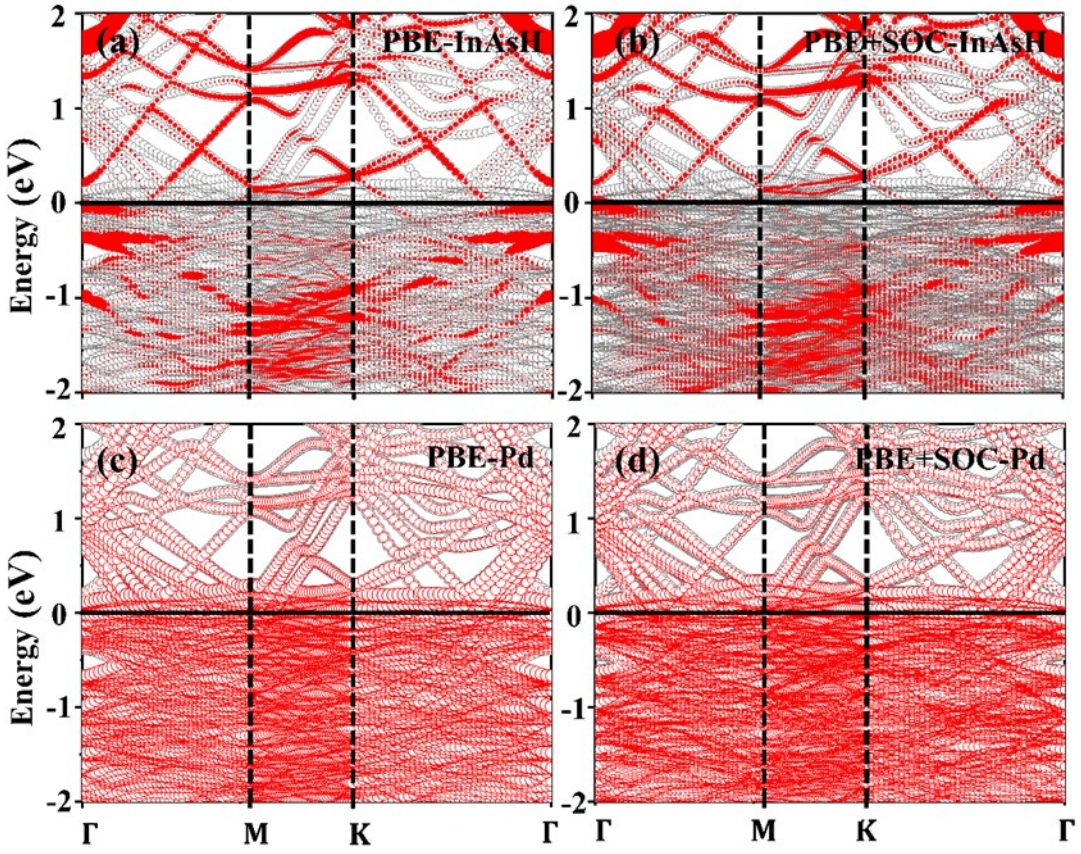

Fig. S5 Band structure calculated : (a) and (c) are the band structures obtained by the Perdew-Burke-Ernzerhof (PBE) method, the red lines represent the projected band structures of (a) ML InAsH and (c) the d orbit of metal Pd, and the gray lines represent the band structures of the InAsHPd complex system. (c) and (d) are the band structures obtained by the PBE+SOC (spin-orbital coupling) method, the red lines represent the projected band structures of (c) ML InAsH and (d) the d orbit of metal Pd, and the gray lines represent the InAsHPd composite system band structures. The Fermi energy level is set to 0 and is indicated by the horizontal black line.

Reference

[1] Kirklin, S.; Saal, J. E.; Meredig, B.; Thompson, A.; Doak, J. W.; Aykol, M.; Rühl, S.; Wolverton, C., The Open Quantum Materials Database (OQMD): assessing the accuracy of DFT formation energies. *npj Computational Materials* **2015,** *1* (1), 15010.

[2] Saiz, F.; Carrete, J.; Rurali, R., Optimisation of the thermoelectric efficiency of zirconium trisulphide monolayers through unixial and biaxial strain. *Nanoscale Advances* **2020,** *2* (11), 5352-5361.

[3] Dai, J.; Yang, T.; Jin, Z.; Zhong, Y.; Hu, X.; Zou, J.; Xu, W.; Li, T.; Lin, Y.; Zhang, X.; Zhou, L., Controlled growth of two-dimensional InAs single crystals via van der Waals epitaxy. *Nano Research* **2022**, *15*, 9954-9959

[4] Li, B.; Yang, Y.; Qi, H.; Sun, Z.; Yang, F.; Huang, K.; Chen, Z.; He, B.; Xiao, X.; Shen, C.; Wang, N., Monolayer $Sc_2I_2S_2$: An Excellent n-Type Thermoelectric Material with Significant Anisotropy. *ACS Applied Energy Materials* **2022,** *5* (6), 7230-7239.